

# Reinforcement learning based deep fuzzy hierarchical clustering to generate personalized non-fungible token artwork

Arman Daliri <sup>a,d,\*</sup> , Nora Mahdavi <sup>a,d</sup>, Mahdieh Zabihimayvan <sup>b</sup>, Aynaz Norouzi Baranghar <sup>c</sup>, Nima Zaeimzadeh <sup>a,d</sup> , Javad mohammadzadeh <sup>a,d</sup>

<sup>a</sup> Department of Computer Engineering, Ka.C., Islamic Azad University, Karaj, Iran

<sup>b</sup> Department of Computer Science, Central Connecticut State University, New Britain, CT, USA

<sup>c</sup> Department of Painting and Sculpture, School of Visual Arts, College of Fine Arts, University of Tehran, Tehran, Iran

<sup>d</sup> Institute of Artificial Intelligence and Social and Advanced Technologies, Ka.C., Islamic Azad University, Karaj, Iran

## ARTICLE INFO

### Keywords:

Digital Arts  
Non-Fungible Token Artwork  
Fuzzy  
Hierarchical  
Deep learning  
Clustering

## ABSTRACT

In the realm of information technology and software development, digital assets increasingly manifest as Non-Fungible Tokens (NFTs) on blockchain platforms, embodying intrinsic material value that enhances user satisfaction. Despite their potential, the creation of NFTs remains costly, time-consuming, and labor-intensive. To address these challenges, we introduce a digital asset generation engine specifically designed for producing NFT artwork. Utilizing real-world datasets curated by digital art experts, our engine synthesizes individual image layers into cohesive, high-quality artistic outputs. Leveraging artificial intelligence, we employ a novel Deep Fuzzy Hierarchical Clustering approach, which integrates autoencoder neural networks, fuzzy clustering, and hierarchical clustering methods. This integrated approach enables precise classification of image layers, achieving an impressive accuracy rate of 95 %. Here, we demonstrate the potential of AI-enhanced solutions in the digital art and NFT space. Our engine not only reduces costs and labor intensity in digital art production but also allows users to personalize their NFT collections by selecting desired layers and specifying rarity, arrangement order, and metadata details. This study underscores the significance of intersectional research between artificial intelligence and fine arts, opening avenues for future advancements in computational art analysis and creative AI applications.

## 1. Introduction

Digital art has rapidly emerged as a transformative form of cultural expression and economic activity in today's world. Blockchain technology has revolutionized the concept of digital ownership, making it possible to create, own and transfer digital assets [1]. NFTs, unique tokens stored on blockchain platforms, represent ownership of a specific digital or physical item [2]. Most NFT collections are usually composed of unique images generated based on random features [3]. The first step in creating an NFT art collection involves creating images, which requires several key steps. Each image is formed by combining a series of layers that are put together randomly (but in a specific order), with each layer containing a distinct attribute. The artist selects a random image from each layer category, stacking them sequentially to form a complete NFT artwork; this is how a single NFT is created.

The initial requirement for creating an NFT Art collection is the layers used in image creation [4]. Each layer category should then create several variations, such as different types of shirts, hats, and so on, which will serve as layers later. Once a sufficient variety of layer categories is created, the artwork is produced by combining these layers [5]. However, most NFT collections today consist of thousands of unique, randomly generated photos [3]. It would be nearly impossible to manually assemble these layers to create each NFT, as this process would take months, and is highly time-consuming [6].

Software programs can perform the entire process of creating NFTs in seconds [7]. These programs take predefined layers as inputs and stack them in a specific order to generate the final images. This process is repeated thousands of times, creating the entire collection in hours rather than months. However, these tools often rely on random combinations of layers and lack the level of control and precision desired by

\* Corresponding author at: Department of Computer Engineering, Ka.C., Islamic Azad University, Karaj, Iran.

E-mail addresses: Arman.Daliri@kiau.ac.ir (A. Daliri), Nora.mahdavi@iau.ir (N. Mahdavi), Zabihimayvan@ccsu.edu (M. Zabihimayvan), Aynaz.norouzi@ut.ac.ir (A. Norouzi Baranghar), N.zaeimzadeh@iau.ir (N. Zaeimzadeh), Javad.mohammadzadeh@iau.ac.ir (J. mohammadzadeh).

artists. One of the traditional techniques to generate art work is based on generative adversarial Networks (GANs). GANs are deep learning architectures, which are widely used for synthesizing audio, image, and video content [8]. Despite their remarkable potential, GANs face limitations in generating high-quality NFT art which closely aligns with an individual's specific artistic vision, particularly when it comes to achieving the necessary precision and high customization. Although the study in [9] reports a promising performance using GANs for generating artwork, the technique used relies on a single architecture model, limiting its adaptability and efficiency in NFT production. Also, the group of volunteers who evaluated the results was not diverse enough and did not include any art specialists/experts.

The broader landscape of digital assets, including NFTs, is also closely connected to emerging virtual environments like the Metaverse, where digital items are shaped by artificial intelligence [10]. Artificial intelligence plays a critical role in generating and interpreting digital images [11], which are fundamental for creating NFTs. AI algorithms can reduce time and costs of producing NFTs, thereby making the process of creating and obtaining them more efficient [12]. However, there are challenges faced, including copyright issues, legal uncertainties, and environmental risks related to energy-intensive blockchain networks [13].

Furthermore, research has also explored using AI for understanding and generating NFT characteristics. For instance, a study [14] investigates NFT and Blockchain through a contextual generative approach to learn the diverse characteristics of NFT collections. It also predicts the potential market value of newly minted NFTs and formulates the generation of predictive transaction series to indicate the future success of new NFT collections. Even though these formulas and predictions work to some degree, due to the dynamic nature of cryptocurrency market, they cannot provide any valuable predictions regarding future collection values and success. Also, a collection's success and value depend on many factors, including the team behind it, the hype around the project, and the quality of the art.

This paper introduces a novel approach with the NFT art generating engine (NFT-AGE), which uses AI-based clustering methods to enhance NFT production. NFT-AGE automates the categorization of image layers, enabling quick generation of customized NFT collections at a high quality. First, a new dataset is designed and created with the help of an art expert. The dataset includes various image layers such as hats, shirts, background, eyes, masks, sunglasses. These layers are then introduced to the engine, where a machine learning system automatically classifies them into distinct categories. The engine uses Deep Fuzzy Hierarchical Clustering (DFH), a method that combines autoencoder neural networks, fuzzy clustering, and hierarchical clustering to sort and categorize the layers. It enables users to customize the order of layers, define the rarity of each layer, and generate metadata file for every NFT. This metadata helps ensure each artwork is unique and cannot be duplicated, while also confirming authenticity and ownership through blockchain technology.

The primary motivation of this research is to provide a long-term and automated method for NFT generation. Initially, the autoencoder performs a general clustering of the data. However, since the autoencoder lacks interpretability and relies on hidden layers in a black-box manner [15], it may lead to inaccuracies in the latent space; therefore, more precise clustering is required to achieve accurate categorization of layers. Subsequently, clustering methods are applied to organize the data so that the main software can properly aggregate them into a final image. Nevertheless, selecting the most suitable clustering method for a given dataset is typically possible only through empirical testing and one-by-one implementation, which is a time-consuming and complex task [16]. To address this, our last optimization technique called World Hyper Heuristic (WHH) is employed to automatically extract two strong candidate methods [17]. WHH selects from a pool of clustering techniques, fuzzy clustering and hierarchical clustering. The integration of fuzzy clustering provides accurate and interpretable categorization of

the previous layers, while hierarchical clustering enables control over the arrangement of image layers for NFT production.

The proposed engine gives artists greater control over both the creative design and technical setup of NFTs, enabling them to produce large collections in less time. Unlike earlier approaches that rely on generative models like GANs, this paper introduces a multi-step clustering approach that integrates AI techniques with artistic input. By combining automation and artistic flexibility, the proposed method offers a more practical and scalable solution for artists and collectors working in the NFT space. The contributions of this work are as follows:

- Proposing a new method for personalizing NFT art using layered image structures.
- Utilizing real-world art layers, designed by experts, to train and test the system.
- Addressing the automatic selection of clustering methods using the World Hyper-Heuristic algorithm, ensuring efficient and accurate NFT layer categorization.
- Introducing a Deep Fuzzy Hierarchical Clustering method by combining autoencoders, fuzzy clustering, and hierarchical clustering for precise image layer classification.
- Enabling users to control layer selection, arrangement, and metadata output.

This paper is organized as follows: 2 examines the history of art and related works. Then, 3 explains and presents the NFT-AGE and its application. In 4, the results are analyzed and reviewed. Finally, in 5, conclusions and future works are presented.

## 2. Literature review

This section gives a comprehensive review of both artistic eras and movements as well as recent works in the field of NFT Art. First, in subsection 2.1, there is a review of art periods and different forms of art in different time series leading up to the production of NFT Art. Then, in subsection 2.2, related works and recently proposed engines for NFT Art production are discussed, along with their respective advantages and disadvantages.

### 2.1. Different time series until the production of NFT art

In this part of the research, different artistic periods and movements are discussed. The studied art periods include Renaissance, Baroque, Neoclassical, Impressionism, Post-Impressionism, Fauvism, Expressionism, Cubism, Futurism, Abstract Expressionism and Pop Art. Finally, the connection between courses and illustration and NFT Art is given. Also, for a better understanding of the artistic time periods studied in this research, in Fig. 1, the examined periods are presented.

Starting with the Renaissance period, when an ideal form was pursued, this era led to the discovery of the golden ratio and improved visual compositions, reflecting the high philosophical ideals of the time [18]. The Baroque period followed, replacing the steady compositions of the Renaissance with dynamic structures and strong contrasts in shadows, producing dramatic pictures [18]. In reaction to Baroque, Neoclassical art emerged, aiming to revive ancient Greek and Roman aesthetics, emphasizing beauty, elegance, and rationality [19]. With Impressionism, artists used vibrant colors and subtle harmonies to depict modern life [18,19], while Post-Impressionists focused on personal expression while still emphasizing structure and form [20]. Fauvism, influenced by Post-Impressionism [21], emphasized bold hue contrasts, while Expressionist artists sought to reveal their personalities and extreme mental states [22].

In response to World War I, Cubism and Futurism arose, with Cubism depicting subjects from multiple angles to uncover their primary reality [23], and Futurism emphasizing simultaneity, movement, and speed as features of modern life [24]. After World War II, Abstract Expressionism emerged, characterized by rhythmic darkness, vivid colors, and a

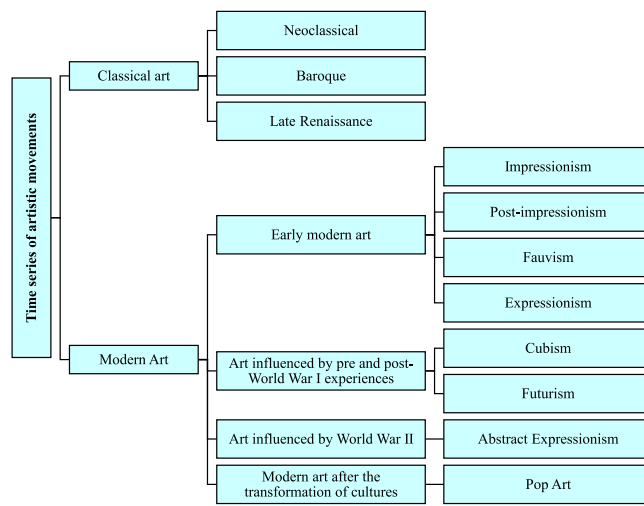


**Fig. 1.** Time series of artistic movements examined in this research.

pursuit of freedom [25]. As social relations shifted, Pop Art integrated fine art with public culture, making it widely accessible and useful in advertising. It reduced the artist's role to that of a designer; its bright colors and mass appeal also influenced illustration [26]. Illustration, although difficult to define, stands between art and graphic design, usually commissioned for specific purposes, with less personal expression but greater accessibility, communication efficiency, and direct message delivery [27].

## 2.2. Related works

This sub section provides a review on the related work and background for this research. First, the relationship between fine arts and NFT Artworks is investigated, and their advantages are recounted. Then, NFT artworks and their creation process are described in detail and the role of AI in digital art and NFT is explained. Finally, recent approaches to NFT creation are reviewed and compared with the performance of the proposed engine. **Table 1** provides a detailed account of the characteristics of the three areas under consideration, highlighting both their

commonalities and distinguishing features. These attributes are elaborated in detail. The inclusion of each feature is marked with an asterisk symbol \* on a green background, while non-inclusion is indicated by an x symbol on a red background.

Illustration involves creating images manually using pencils, colored pencils, watercolors, gouache, and other art materials [27]. However, many painters and designers today prefer to use software such as Adobe Illustrator or Photoshop for digital design. Illustration is typically used as a form of drawing or picture alongside a text or story. To become an illustrator, one must transform concepts and ideas into an understandable and engaging image. This requires proficiency in different styles and techniques, including painting, cartoon drawing, digital painting, and other artistic styles [27].

The specialized features of fine arts include mastery of both traditional and modern painting techniques, use of colors, composition of shapes, and attention to detail [28]. Fine art artists should be familiar with using different tools such as colored pencils, oil painting, watercolors, and pencils. They should also be able to interpret human, social, and cultural concepts in their work in order to establish an artistic value and meaning. Achieving mastery over the combination and balance of designs and colors requires deep knowledge and understanding of color theory, forms, and artistic patterns in an art work. Fine-art artists must have the ability to be highly creative and express their personality in the work [28].

Moving NFT Art utilizes blockchain technology to create tradable and permanent data for each artwork. These works of art are created digitally using art software and different technologies [29]. NFT Art includes various types of digital media such as 3D images, videos, music, and other art forms. Unlike traditional art, NFT Art is tradable as a digital asset whose authenticity and ownership are guaranteed by blockchain technology. Due to its digital nature, NFT Art actively interacts with online communities and can influence and be significant in the digital world [29].

### 2.2.1. Fine arts and NFT artworks

Based on research, the NFT art industry has become a beautiful cycle due to the connection between artists and NFT fans [30]. A collector may join a Discord channel of an NFT project or follow an artist or collector's account to share opinions and receive updates directly from content creators [31]. Virtual worlds such as Metaverse have been

**Table 1**

Detailed account of the characteristics of the three areas under consideration and identifies their commonalities and distinguishing features.

Features	Topics	NFT Art	Fine Arts	Illustration
Ability to interpret and create artistic value		x	*	x
Ability to prove authenticity and ownership		*	*	*
Ability to work with different styles and techniques		x	x	*
Artistic value		*	*	*
Being digital		*	x	*
Communication with technology		*	x	*
Communication with the Internet community		*	x	x
Creativity and artistic originality		*	*	*
Creativity and self-expression		x	*	x
Cultural influence		*	*	*
Diversity in media		*	x	x
Focus on visualizing ideas and concepts:		x	*	*
Imaginary drawing and painting skills		x	*	*
Mastering the combination and balance of designs and colors		x	*	*
Relative to anecdotes and narratives		x	*	*
Using blockchain technology		*	x	x
Using different art tools		x	*	x
Using digital software		x	x	*
Using hand painting and drawing techniques		x	*	*

developed in response to interests in the NFT supply and demand market [32]. Metaverse and NFT Artworks enable users to create digital images for a wide variety of applications, including video games, marketing, and advertisement.

While both fall under the umbrella of visual arts, there are distinct differences between illustration and fine arts [33]. Illustration is typically used to convey or clarify a particular concept, often in a more practical sense, such as books or visual media [34]. On the other hand, fine arts are created to express an artist's original, emotional, or philosophical ideas, with aesthetics being the primary focus [35]. While illustration may sometimes be limited by commercial considerations or publishers' guidelines, the boundary between illustration and fine art has become increasingly blurred [36]. With artists like Norman Rockwell, who combine technical skill with personal insight, we can see a fusion of these two art forms [37].

The commonalities between illustration and fine art can be explored through various aspects, such as technical skills, visual principles, and creative logic. However, they differ in their purpose and execution [38]. Regarding technical and instrumental skills, both fields rely on the same fundamental abilities in painting, drawing, and other visual forms, including mastering perspective, color, and composition [39]. In terms of visual principles, both arts utilize the basic principles of visual order like balance, repetition, contrast, emphasis, and unity, which are crucial in creating their works [40]. In creative logic, artists in both fields seek to innovate and create, whether through visual metaphors, defying convention, or experimenting with form and content. As time passes, many illustrators, such as Salvador Dali or Andy Warhol, have transcended the limits of mere illustration into fine art by creating works which are displayed and admired in museums and galleries. Ultimately, the similarity between illustration and fine arts lies in the foundation of visual creation and the creative expression of artists, even though the purpose of creating works may differ [40].

### 2.2.2. Non-fungible token artwork

Various specialized ways exist to explore the relationship between imagery and NFT artifacts. By tokenizing works, illustration and registering them on blockchains, each piece is assigned a unique digital ID that enables verification of ownership and digital authenticity. While Digital Validity Images have existed in the digital world for some time, offering them as NFTs elevates their status from copyable images to valuable and unique works of art in the digital marketplace [41]. The new capabilities provided by NFTs offer a new market for visual artists, allowing them to track transactions and ownership over time and earn a percentage of each resale. With NFTs, visual artists can bypass traditional channels and artistic intermediaries to directly reach communities of enthusiasts and collectors. The innovative attractiveness in illustration can create new revenue streams to explore new opportunities in digital art by innovating and creating works that integrate well with the NFT format [41]. Imagery NFTs, especially those with interactive and experiential elements, can gain prominence in online communities and create more significant interaction and dialogue between artists and audiences. Thus, the combination of imaging and NFTs in the digital age can enable artists to create new experiences for collecting, owning, and sharing their artwork [41].

Creating and distributing an artwork as an NFT involves a detailed and standardized process [30]. The first stage is ideation and content production, which entails producing digital content, such as images, animations, videos, and other art forms, with an innovative and unique approach. The emphasis is on originality and creativity, which are critical to the creation of any NFT [42]. The second stage is technical preparation, which involves reviewing the digital file to ensure it is of appropriate quality and format, such as PNG, GIF, or MP4. The third stage is choosing the blockchain. Identifying an appropriate blockchain such as Ethereum, Tezos, Flow, Binance Smart Chain, to register the NFTs is the main pillar of the entire process [43]. The fourth stage is preparing a digital wallet, which is necessary to store and exchange

NFTs. Prominent wallets such as Meta Mask, Trust Wallet, and Coinbase Wallet, provide the necessary facilities in this field [44].

In the fifth stage, a distribution platform is selected, and the artwork is offered as an NFT on specific platforms such as OpenSea, Rarible, Foundation, or SuperRare [45]. Each of these platforms has unique advantages and characteristics. The sixth stage involves the "Minting" operation, which focuses on fixing the Artwork as NFT on the blockchain. This practice may be accompanied with the costs associated with blockchain transactions, known as "Gas Fees" [46]. The seventh stage sets sale characteristics by determining the price and deciding whether to sell by auction or at a fixed price. Some unique properties can also be assigned to each NFT [47]. The eighth step is marketing and promotion, which encompasses marketing activities after NFT registration, including using social media, email campaigns, advertising on relevant networks, and other marketing strategies to increase reputation and attract buyers. In practice, the creation and design of an NFT artwork and its promotion to successful sales require not only technical knowledge and skills but also a deep understanding of the market, blockchain technology, and legal issues related to copyright and business strategies [29].

### 2.2.3. Metaverse and similar works

Artificial Intelligence (AI) is the fundamental technology used in both blockchain and Metaverse. AI in the field of NFTs is a simulation of human intelligence used to analyze and recognize input images and to produce poems and images by processing related phrases and words [48]. Ensuring thematic coherence in images and managing different word frequency are two important issues that should be considered in using AI for NFT [49]. Audiovisual spaces created in Metaverse to write and perform music are similar to studios and halls for artists. The use of such virtual spaces for holding concerts allows more interaction between audience and artists.

Among all different markets and software programs related to NFT, AI has come into play to ease the production process. Since creating NFTs is very profitable but time-consuming, using GANs to produce NFTs more efficiently is one of the available solutions [9]. The study in [9], which works based on style transfer, uses a Kaggle dataset of 2283 images to train a GAN model. After training, the produced works are measured qualitatively and quantitatively using Fréchet Inception Distance (FID) and Kernel Inception Distance (KID) criteria [50]. The results show that the created images are comparable with the original examples of images in terms of quality, which attracts other researchers to conduct more study in this field [51]. The work in [5] investigates the ability of GAN models and deep learning in NFT creation, analyzing the generated images using a Style-GAN model to edit visual features.

To better understand the value of GANs in this context, it is essential to examine their structure and functionality. Generative Adversarial Networks (GANs) are a subcategory of Generative Networks with the ability to create new data samples with similar patterns to training data [52]. They were first introduced in 2014, marking a leap for generative models in computer vision. Traditional networks applying methods such as texture synthesis and texture mapping, were less effective than GANs in producing diverse images [53]. As a powerful model, GANs self-learn and self-generate new synthetic data mirroring real-world data [54]. Due to their progress in recent years, they have been widely applied in different domains such as computer vision, video and image processing, healthcare and stock market [55].

A typical GAN architecture consists of two modules named the Generator and the Discriminator. The Generator is an unsupervised module that learns the probability distribution of training data and generates synthetic data using a random noise vector. The Discriminator is a binary classifier which differentiates generated samples from real ones by assigning them labels of 0 and 1 [54]. The generator tries to fool the discriminator and their competition results in overall better performance of the model. GAN follows a min-max loss function where the generator wants to minimize the loss and the discriminator aims to

maximize it. Backpropagation is used to update both the generator and the discriminator's parameters during the training process. The ultimate goal is for the Generator to produce synthetic data similar to real samples while the discriminator improves in distinguishing between real and fake data generated by the Generator [52].

### 3. Proposed non-fungible token artwork generating engine (NFT-AGE)

In this section, we discuss our proposed engine, called NFT-AGE, in detail. In subsection 3.1, the general process flow of the NFT-AGE is discussed and in subsection 3.2, clustering method and creation process for NFT Artwork are explained. Finally, flowchart for NFT-AGE is presented, with additional explanatory details.

#### 3.1. NFT-AGE overview

As shown in Fig. 2, NFT-AGE consists of 4 steps. Step 1, Cluster Step, includes reading the database and clustering the layers. Step 2, Selection Step, is where the user can set the designed combination according to the clustering done by the engine. In step 3, Creation Step, the engine produces NFT artworks. Finally, in step 4, Output Step, all NFTs are stored in a user-specified storage.

In *Cluster Step* (Step 1), the engine reads the data. The dataset created and used in this work includes designed layers of the hat, face, sunglasses, mask, shirt and background. A machine learning system, which is designed for this part of the engine, automatically categorizes all the layers and prepares them for the next step. For example, the system

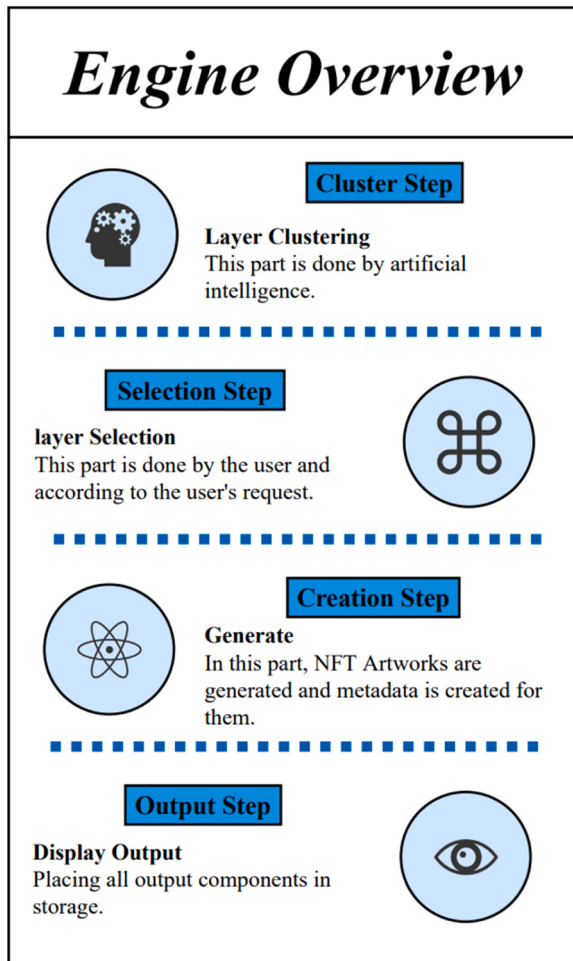


Fig. 2. Engine overview.

reads all the hat layers and automatically classifies them into "new" or "old" categories. The user can further select and customize the NFT Artwork by sorting layer categories.

In *Selection Step (Step 2)*, the layers have been categorized by the machine learning system, the user specifies the storage location of the output files on their device. The user can also select the desired number of NFT Artworks to generate. Features such as image size and the project name can be customized to personalize the NFT collection. After these configurations, the user selects the desired layers according to the categories and issues the build command to initiate the creation process.

In *Creation and Output Steps (Step 3 and 4)*, executing the user's commands, the engine processes the images and generates metadata for each generated image. Any produced metadata is used within the blockchain network to convert an image into an NFT Artwork. Also, the metadata is utilized to prevent the reproduction of an image formerly created in this engine. If duplicate metadata is generated, repetition is prevented, and another image will be created. Next, the image production and the stop conditions for the final creation of NFT Artwork are checked, and the images and metadata are finally prepared and saved in the user's designated folder.

#### 3.2. Implementation of NFT-AGE clustering (deep fuzzy hierarchical clustering)

Fig. 3 presents an overview of the clustering step in NFT-AGE. Image layers are clustered using a novel technique called Deep Fuzzy Hierarchical Clustering (DFH). DFH integrates three clustering methods in

#### Implementation of NFT-AGE clustering

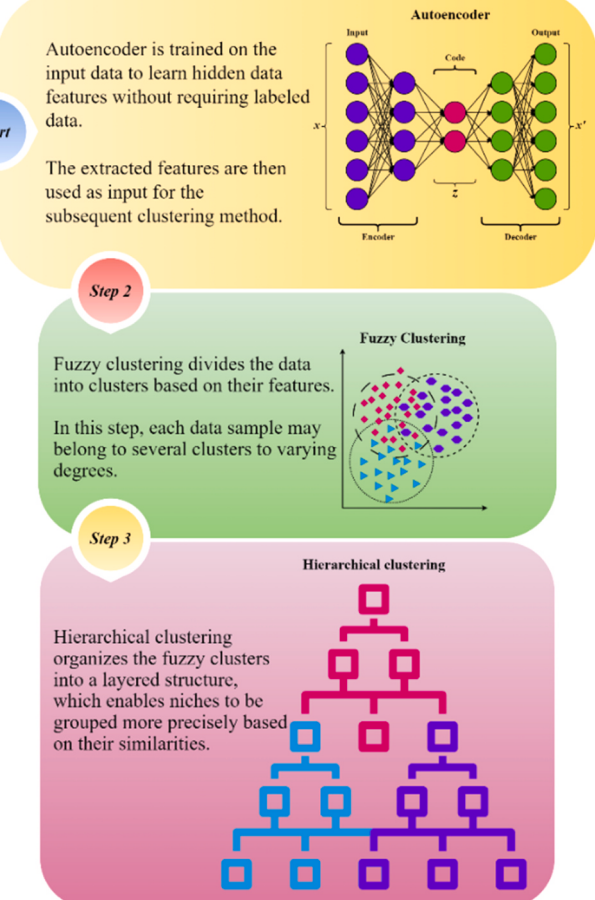


Fig. 3. Implementation of NFT-AGE clustering (Deep Fuzzy Hierarchical Clustering-DFH).

order: (1) An autoencoder deep neural network [56,57], (2) Fuzzy Clustering [58], (3) Hierarchical clustering [59]. DFH Clustering was selected based on the World Hyper Heuristic (WHH) algorithm [17], a well-known reinforcement learning method for dynamically exploring and exploiting the search space in algorithm selection problems [17,60]. Although originally presented to optimize the selection of metaheuristic algorithms for Np-hard problems [17,61], in this article we implemented the WHH algorithm to select the best matching clustering algorithm. For this purpose, in addition to the finalized algorithms, we implemented eight other algorithms within WHH, which are: K-means [62], Affinity Propagation [63], Mean Shift [64], Spectral Clustering [65], DBSCAN [66], OPTICS [67], Gaussian Mixture Clustering [68], and BIRCH [69]. 4 provides detailed information on the results of our comparison.

WHH introduces a reinforcement learning (RL) approach designed to enhance the search problem through adaptive decision-making. This technique dynamically balances exploration and exploitation by leveraging multiple algorithms, each adjusted according to evolving RL-based criteria. The selection of exploration and exploitation strategies varies iteratively, ensuring tailored solutions for distinct problem states. At each algorithmic iteration, the model refines its search methodology, distinguishing itself from conventional approaches by continuously adapting its strategy. The RL framework enables the system to consistently prioritize optimal clustering techniques in every iteration, mitigating the risk of overlooking potentially effective clusters—a common limitation in greedy metaheuristic algorithms. The process operates in two key phases: reward evaluation and algorithm selection. Initially, the system estimates the expected efficacy of each clustering algorithm for subsequent iterations. Following this assessment, it selects the most promising clustering strategy to guide exploration and exploitation in the next cycle.

The reward evaluation phase for clustering algorithms establishes an impartial benchmarking framework, ensuring equitable performance assessment across all available methods. During the initial iteration, every cluster processes the same randomly generated solution population to identify an optimal outcome. For instance, in a basic minimization task defined by  $f(x)$ , where  $x \in R$  and  $f : R \rightarrow R$ , the  $i^{th}$  cluster begins with  $m$  arbitrary solutions  $\{Z_1, Z_2, Z_3, \dots, Z_m\} \in R$ . Through iterative refinement, it converges to  $L_i \in R$  as the locally optimal solution. The results of these population-based algorithms are aggregated into an array  $gpopCostA = \{L_1, L_2, \dots, L_i\}$ , where  $i \in [1, n]$  and  $n$  denotes the total number of clusters. Subsequently, the most effective algorithm for minimizing  $f(x)$  is determined by computing the reward values stored in the array  $AlgReward$ , as formalized in Eq. 1.

$$AlgReward = 1/gpopCostA \quad (1)$$

To ensure rapid and effective convergence, the selection phase of the RL method utilizes  $AlgReward$  as a heuristic guide. This approach systematically explores potential solutions within an uncertain search space while maintaining computational efficiency by executing only one cluster per iteration. The heuristic is dynamically refined based on iterative findings, ensuring adaptive optimization. A pivotal component of this process is the learning rate parameter,  $RLAlpha$ , which governs the balance between exploration and exploitation. Initially set to zero to ensure unbiased algorithm selection,  $RLAlpha$  adjusts incrementally with each iteration. In reinforcement learning, the learning rate is typically tailored to specific application requirements, often depending on factors such as elapsed time or iteration count. Empirical testing revealed optimal performance when  $RLAlpha$  is constrained within the range [1,10].

As formalized in Eq. 2,  $RLAlpha$  increments by  $1/\text{maximum iterations}$  per cycle, maintaining bounds within [0, 10]. This progressive adjustment shifts the selection bias toward algorithms with higher  $AlgReward$  values, emulating a roulette wheel mechanism that favors top-performing methods. Experimental results demonstrate that this configuration achieves peak efficiency, with  $RLAlpha$  values in [0, 10]

fostering a diversified search in early stages and intensified exploitation in later phases. To further regulate the transition between exploration and exploitation, the method incorporates a stochastic control variable, choose-random, sampled uniformly from [0, 1] in each iteration. If choose-random falls below  $RLAlpha$ , then the roulette wheel selection prioritizes high-reward algorithms. Additionally, the system monitors optimization progress: if no improvement occurs over two consecutive iterations, the leading algorithm's reward is penalized by the average reward of alternative methods (Eq. 3). These safeguards prevent convergence to suboptimal local minima and mitigate resource starvation in advanced iterations.

$$RLAlpha = RLAlpha + (1/\text{maximum iterations}) \quad (2)$$

$$AlgReward_i = AlgReward_i - \frac{\left(\sum_{j=1}^{j \neq i} AlgReward_j\right)}{n} \quad (3)$$

To extract patterns and organize the data, DFH operates in three sequential steps. First, the autoencoder deep neural network is trained on the input data to learn hidden data features without requiring labeled data. The extracted features are then used as input for the subsequent clustering method. Fuzzy clustering divides the data into clusters based on their features. In this step, each data sample may belong to several clusters to varying degrees. Finally, hierarchical clustering organizes the fuzzy clusters into a layered structure, which enables niches to be grouped more precisely based on their similarities.

WHH receives a pool of candidate clustering algorithms, including finalized methods and alternative algorithms such as K-means, DBSCAN, and Gaussian Mixture, as input. The input data, consisting of NFT image layers, is initially processed using a randomly generated solution population, and the performance of each algorithm in accurately categorizing the layers is evaluated. This approach allows for a comprehensive and unbiased exploration of the algorithmic search space.

Subsequently, reinforcement learning evaluates the performance of the clustering algorithms, with reward values determined in each iteration based on the collected results. The most effective algorithms are then selected for the next phase, and in the case of DFH, fuzzy and hierarchical clustering are applied sequentially. First, the autoencoder extracts latent features from the data. Then, fuzzy clustering classifies the data using soft assignments, and finally, hierarchical clustering organizes these clusters into a layered structure.

The rationale for selecting these three algorithms lies in their complementary roles. The autoencoder is employed to extract compact latent features from high-dimensional NFT image layers, enabling more efficient data representation. Fuzzy clustering is then applied, as it is well-suited for handling noisy and overlapping data by assigning samples to multiple clusters with varying degrees of membership. Finally, hierarchical clustering provides a layered organization of clusters, which aligns with the multi-level structure of NFT image composition.

Autoencoders are used to learn efficient data representations without precise labels. Autoencoders aim to extract essential and hidden features of data and display them more compactly. These networks consist of two main parts: the Encoder part, which converts the input into a compressed representation, and the Decoder part, which returns this compressed representation to an approximation of the original input. This process allows the network to automatically learn essential patterns from the data without labels.

Given input  $x$ , the encoder is defined as a function that converts  $x$  into a hidden space or representation with fewer dimensions,  $z$ . (Eq. 4). The Decoder is another function that returns this hidden representation  $z$  to an output almost identical to the original input  $x$ . (Eq. 5). Autoencoder training aims to optimize the parameters  $\theta$  and  $\phi$  so that the output reconstruction value  $x'$  is close to  $x$ . In other words, the goal is to minimize the reconstruction function ( $L(x, x')$ ).

$$z = f\{\theta\}(x) \quad (4)$$

$$x' = g\{\phi\}(z) \quad (5)$$

In the next step, fuzzy clustering is applied to the data. Based on the information from the dataset, the clustering algorithm provides a classification for the layers. Fuzzy clustering is an algorithm that divides data into clusters where each data point belongs to each cluster to a certain degree. In this algorithm, the number and centers of the clusters should first be specified by an expert. The performance of this method strongly depends on the initial number of clusters and the initial locations of the cluster centers [70]. The purpose of fuzzy clustering is to extract fuzzy models from the data. The steps of the fuzzy clustering algorithm are as follows:

1. Determine the number of clusters in a data set.
2. Randomly assign each data point to its corresponding cluster.
3. Repeat clustering to cover all data in closer clusters.
4. Calculate the cluster center of each cluster.
5. Detect the presence of any data in any cluster.

**Eq. 6** indicates the formulation of the fuzzy clustering algorithm, where  $n$  is the number of data points,  $m$  is the fuzziness index, and  $m$  is a member of  $[1, \infty]$ .  $\mu_{ij}$  represents the membership of its data to the  $j^{\text{th}}$  cluster center.  $v_j$  represents the  $j^{\text{th}}$  cluster centre, and  $c$  represents the number of the cluster center. Also,  $d_{ij}$  represents the Euclidean distance between its data and the  $j^{\text{th}}$  cluster center. The formulation of the distance between centralities and clusters is shown in **Eq. 7**, where  $\|x_i - v_j\|$  is the Euclidean distance between its data and the  $j^{\text{th}}$  cluster center.

$$\mu_{ij} = 1 / \left( \sum_{k=1}^c \left( \frac{d_{ik}}{d_{ik}} \right)^{\frac{2}{m-1}} \right)$$

$$v_j = \left( \sum_{i=1}^n \left( \mu_{ij} \right)^m x_i \right) / \left( \sum_{i=1}^n \left( \mu_{ij} \right)^m \right), \quad \forall j = 1, 2, \dots, c \quad (6)$$

$$J(U, V) = \sum_{i=1}^n \sum_{j=1}^c \left( \mu_{ij} \right)^m \|x_i - v_j\|^2 \quad (7)$$

Hierarchical clustering falls into two categories: top-down and bottom-up. Bottom-up algorithms first treat each data point as a single cluster and then successively merge pairs of clusters until all clusters integrate in a single cluster, which includes all data points. Hence, bottom-up hierarchical clustering is known as Hierarchical Aggregation Clustering (HAC), and the results are often visualized using a tree (or dendrogram).

The tree's root is a unique cluster that collects all instances; the leaves represent individual data instances. The average linkage method in this algorithm is computed with **Eq. 8**.  $Trs$  is the sum of all pairwise distances between cluster  $r$  and cluster  $s$ .  $Nr$  and  $Ns$  are the sizes of the clusters  $r$  and  $s$ , respectively. At each hierarchical clustering stage, the clusters  $r$  and  $s$  are merged, for which  $D(r, s)$  is the minimum.

$$D(r, s) = Trs / (Nr * Ns) \quad (8)$$

The most important part of the engine is to perform precise clustering, which is objectively based on the engine's output. Also, to better interpret the cluster outputs, its numerical results are presented using the criteria of the confusion table. To summarize the entire process, **Fig. 4** indicates the flowchart of the proposed engine.

#### 4. Experimental evaluation

As mentioned earlier, several different layers corresponding to image components are clustered. Some examples of the layers used in the engine, which include a hat, face, sunglasses, shirt, and background, are shown in **Fig. 5**. NFT-AGE can cluster layers like the ones shown in **Fig. 5**

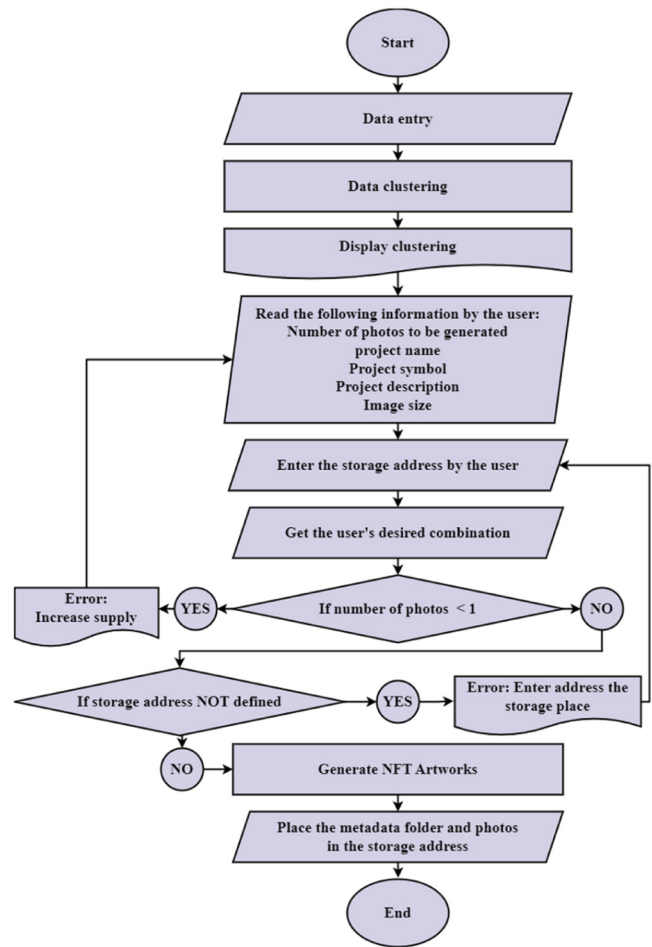


**Fig. 4.** Flowchart of the NFT-AGE.

and assemble them into a complete image. The results of clustering and classification algorithms extracted from each of the final images is discussed in this section.

In **3**, Fuzzy clustering, applied in step 1 of the engine is selected based on a comparison with 8 other clustering techniques, which are listed in **Table 2**. The parameter settings for each algorithm are also provided.

The criteria of accuracy, precision, recall, and F1 score are used to evaluate and compare the clustering algorithms (**Eqs. 9–12**). In these Equations,  $N$  represents the size of the adversarial class,  $TP$  refers to the number of samples that are in the positive class,  $TN$  refers to the number of samples that are in the negative class,  $FP$  is the number of samples incorrectly classified as positive, and  $FN$  is the number of samples mistakenly classified as negative [71].

$$\text{Accuracy} = \frac{TP + TN}{P + N} \quad (9)$$

$$\text{Precision} = \frac{TP}{TP + FP} \quad (10)$$

$$\text{Recall} = \frac{TP}{TP + FN} \quad (11)$$

$$\text{F1-score} = \frac{2TP}{2TP + Recall} \quad (12)$$

**Figs. 6–9** displays the results obtained from the implementation of the algorithms. The best result was achieved by DFH, with an accuracy of 95 %. It is worth mentioning that DFH is the only algorithm that produced identical values across all evaluation metrics used in our comparisons. According to the analysis of the extracted results, due to

Background	Shirt	Face, sunglasses, Mask	Hat

Fig. 5. Image layers.

the order of the dataset, each algorithm generated specific and consistent values for each output criterion. Based on these collected results, the selected algorithm for this version of the proposed fuzzy clustering algorithm engine was chosen. In the following, the output of the images and their correlation with the clustering process are discussed.

Based on the provided precision values in Fig. 6 for each clustering algorithm, DFH achieves the highest precision (92 %), outperforming all other methods, followed by Affinity Propagation and DBSCAN (88 %). Gaussian Mixture and k-means exhibit identical performance (83 %), while Spectral clustering shows slightly lower precision (82 %). Mean Shift, OPTICS, and BIRCH demonstrate the weakest performance among the compared algorithms, with BIRCH being the least precise (78 %). These results suggest that DFH is the most effective algorithm for this specific clustering task, whereas BIRCH may require further optimization or may be less suitable for the given dataset. The middle-tier algorithms (Gaussian Mixture, k-means, and Spectral) offer moderate performance, making them viable alternatives depending on computational or application-specific constraints.

The recall results (Fig. 7) demonstrate that DFH again achieves the highest performance (95 %), indicating its superior ability to correctly identify relevant clusters compared to other algorithms. Affinity Propagation and DBSCAN follow closely with 90 % recall, reinforcing their

robustness in capturing true positives. Gaussian Mixture and k-means exhibit identical recall (85 %), mirroring their precision trends, while Spectral clustering shows slightly lower recall (84 %). Mean Shift and OPTICS share the same recall (82 %), suggesting comparable limitations in coverage, whereas BIRCH remains the weakest performer (80 %). Combined with the precision analysis, DFH emerges as the most balanced and effective algorithm, excelling in both precision (92 %) and recall (95 %). The consistency between precision and recall for Gaussian Mixture, k-means, and DBSCAN highlights their reliability, whereas BIRCH's low scores across both metrics warrant reconsideration of its suitability for this task. These findings underscore the importance of evaluating both precision and recall to comprehensively assess clustering performance.

The F1-score results (Fig. 8), which harmonize precision and recall into a single metric, further solidify DFH's dominance with a score of 95 %, reflecting its exceptional balance between precision (92 %) and recall (95 %). This indicates that DFH not only minimizes false positives but also maximizes true positives, making it the most reliable algorithm for this clustering task. Affinity Propagation and DBSCAN again perform strongly with an F1-score of 89 %, aligning with their high precision (88 %) and recall (90 %), which suggests consistent performance across both metrics. Gaussian Mixture and k-means maintain their parity with

**Table 2**

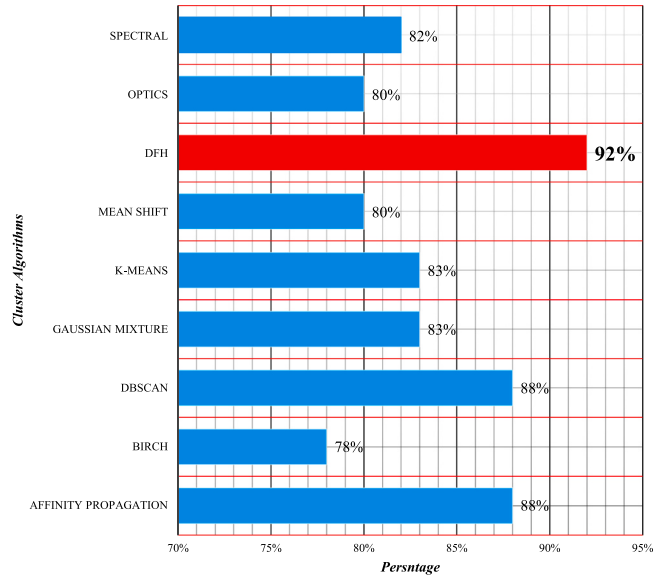
The parameters of Clustering algorithms.

Algorithm	Parameters
k-means clustering [72]	n_clusters= 8, init= 'k-means++', n_init= 'auto', max_iter= 300 tol= 0.0001 verbose= 0 random_state=None copy_x=True algorithm= 'lloyd' damping= 0.5 max_iter= 300 convergence_iter= 15 copy=True, preference=None affinity= 'euclidean' verbose=False random_state=None bandwidth=None seeds=None bin_seeding=False min_bin_freq= 1 cluster_all=True n_jobs=None max_iter= 300 n_clusters= 8 eigen_solver=None n_components=None random_state=None n_init= 10 gamma= 1.0 affinity= 'rbf' n_neighbors= 10 eigen_tol= 'auto' assign_labels= 'kmeans' degree= 3 coef0= 1 kernel_params=None n_jobs=None verbose=False eps= 0.5 min_samples= 5 metric= 'euclidean' metric_params=None algorithm= 'auto' leaf_size= 30 p = None n_jobs=None min_samples= 5 max_eps=inf metric= 'minkowski' p = 2 metric_params=None cluster_method= 'xi' eps=None xi= 0.05 predecessor_correction=True min_cluster_size=None algorithm= 'auto' leaf_size= 30 memory=None n_jobs=None n_components= 1 covariance_type= 'full' tol= 0.001 reg_covar= 1e-06 max_iter= 100 n_init= 1 init_params= 'kmeans' weights_init=None means_init=None precisions_init=None random_state=None warm_start=False verbose= 0 verbose_interval= 10
Affinity propagation clustering [63]	
Mean Shift clustering [64]	
Spectral clustering [65]	
DBSCAN clustering [66]	
OPTICS clustering [67]	
Gaussian mixture clustering [68]	

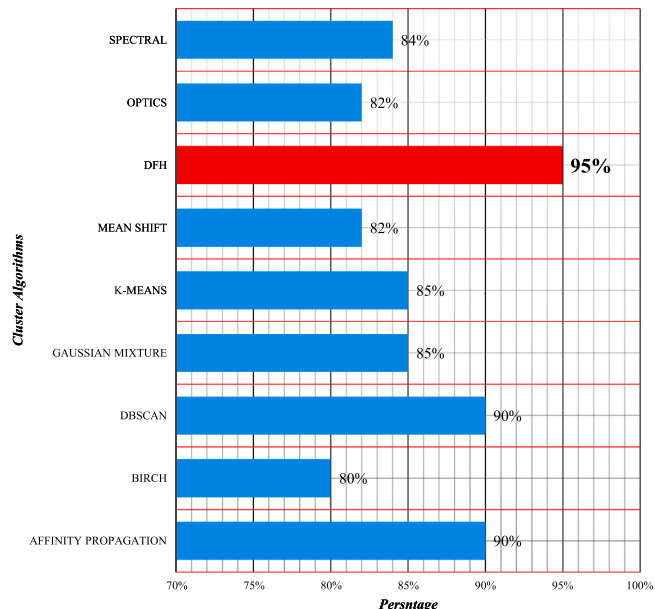
**Table 2 (continued)**

Algorithm	Parameters
BIRCH clustering [69]	threshold= 0.5 branching_factor= 50 n_clusters= 3 compute_labels=True copy=True

## Precision

**Fig. 6.** Precision results obtained from the implementation of the clustering algorithms.

## Recall

**Fig. 7.** Recall results obtained from the implementation of the clustering algorithms.

an F1-score of 84 %, mirroring their precision (83 %) and recall (85 %), highlighting their stable but middling effectiveness. Meanwhile, Spectral clustering's F1-score (82 %) is slightly lower, consistent with its

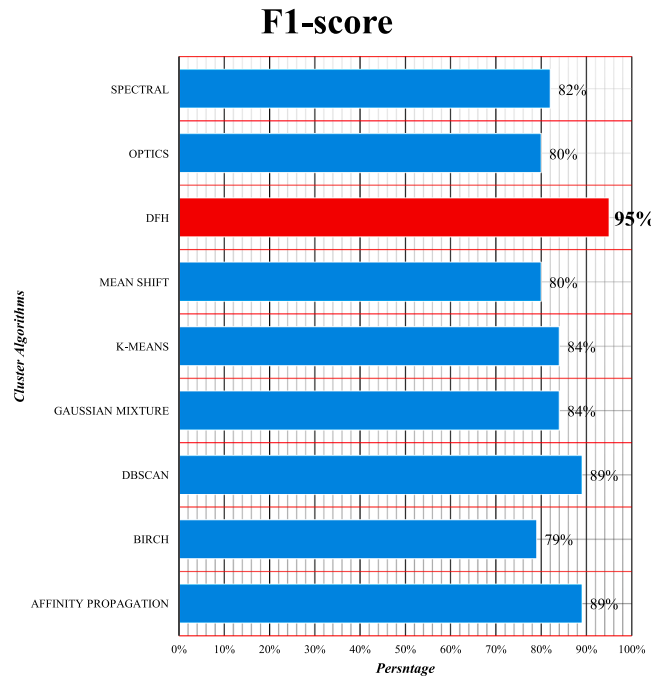


**Fig. 8.** F1-score results obtained from the implementation of the clustering algorithms.

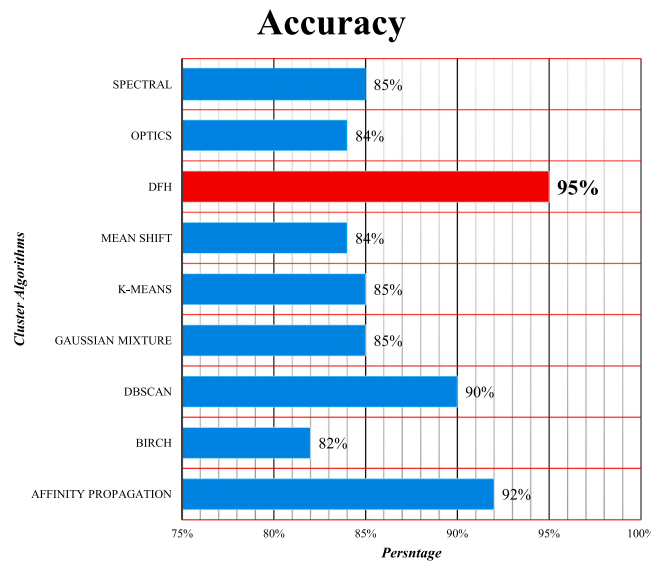


**Fig. 9.** Accuracy results obtained from the implementation of the clustering algorithms.

marginally weaker precision (82 %) and recall (84 %), indicating a minor trade-off between accuracy and coverage.

The lower-tier algorithms, including Mean Shift, OPTICS, and BIRCH, exhibit F1-scores of 80 %, 80 %, and 79 %, respectively, which align with their subpar precision and recall results. BIRCH, in particular, lags behind in all metrics (precision: 78 %, recall: 80 %, F1-score: 79 %), underscoring its limitations for this application. The strong correlation between F1-scores and the earlier precision/recall values reinforces the validity of these findings: DFH excels comprehensively, while BIRCH consistently underperforms. This holistic analysis emphasizes that F1-score is a critical metric for evaluating clustering algorithms, as it captures the interplay between precision and recall, revealing which methods strike the optimal balance for practical deployment.

The accuracy results in Fig. 9 provide further confirmation of DFH's superior performance, achieving 95 % accuracy, which is the highest among all evaluated algorithms. This aligns perfectly with its top-tier precision (92 %), recall (95 %), and F1-score (95 %), demonstrating comprehensive excellence across all evaluation metrics. Affinity Propagation maintains its strong performance with 92 % accuracy, closely matching its high precision (88 %) and recall (90 %), though its slightly lower precision suggests it may produce marginally more false positives than DFH. DBSCAN shows a small dip in accuracy (90 %) compared to its F1-score (89 %), which could indicate minor inconsistencies in its clustering behavior despite generally reliable performance.

Gaussian Mixture, k-means, and Spectral clustering all achieve comparable accuracy (85 %), mirroring their similar precision (83–84 %) and recall (85 %) scores. This consistency suggests these algorithms are stable but unexceptional choices for this task. Mean Shift and OPTICS again perform identically (84 % accuracy), reinforcing their mid-to-lower-tier status, as seen in their precision (80 %) and recall (82 %). BIRCH remains the weakest performer (82 % accuracy), consistent with its poor results across precision (78 %), recall (80 %), and F1-score (79 %). The strong correlation between accuracy and earlier metrics underscores DFH's robustness, while BIRCH's consistently low scores highlight its limitations. These results emphasize that accuracy alone can be a reliable indicator of overall performance when supported by complementary metrics like precision and recall.

In order to comprehensively evaluate the performance of clustering algorithms, it is imperative to employ multiple evaluation criteria that can provide a more accurate and thorough understanding of the proposed method. In this section, we have used three distinct evaluation criteria to assess the performance of the proposed method. By employing these criteria, we aim to provide a reliable and comprehensive evaluation that can assist in making informed practical or academic decisions.

The Calinski-Harabasz method uses a clustering algorithm to determine appropriate classes within a dataset [73]. This method calculates the Calinski-Harabasz index as the ratio of between-cluster dispersion to the sum of within-cluster dispersion for each cluster. A higher value of this metric indicates denser and more distinct clusters. Eq. 13 presents the mathematical formulation of the Calinski-Harabasz index. If the dataset  $E$  contains  $n_E$  elements and is divided into  $k$  clusters, the Calinski-Harabasz index, denoted as  $s$ , is calculated as the ratio of between-cluster dispersion to within-cluster dispersion. In this context,  $W_k$  represents the within-cluster scatter, and  $B_k$  denotes the between-cluster scatter. The Calinski-Harabasz index is defined as the ratio of the mean between-cluster variance to the mean within-cluster variance, that is,  $\frac{tr(B_k)}{k-1}$  for the between-cluster component and  $\frac{tr(W_k)}{n_E-k}$  for the within-cluster component. Dividing these two quantities yields Eq. (13).

However, for the derivation of Eq. 13, it is assumed that we have  $E = \{x_1, x_1, \dots, x_{E^n}\}$  and each  $x_i$  is a feature vector. In this case, the total dispersion matrix is equal to Eq. 14, where  $\bar{x}$  is the mean of the entire data and this matrix represents the total variance and covariance of the data. The data is then divided into  $k$  clusters. The dispersion of the data of each cluster relative to the center of the same cluster is  $W_k$  and the dispersion of the centers of the clusters relative to the total mean is  $B_k$ . This means that the total dispersion is equal to the sum of the intra-cluster dispersion and the inter-cluster dispersion  $T = W_k + B_k$ . Then, to show the total dispersion between or within clusters, the Trace matrix  $B_k$  and  $W_k$  are taken. The between-cluster dispersion matrix, defined in Eq. 15, is traced by  $tr(B_k)$  while  $tr(W_k)$  traces the within-cluster dispersion matrix defined in Eq. 16.  $C_i$  represents the center of cluster  $i$ , and  $n_q$  is the number of points in cluster  $q$  [73].

$$s = \frac{tr(B_k)}{tr(W_k)} \times \frac{n_E - k}{k - 1} \quad (13)$$

$$T = \sum_{i=1}^{E^n} (\mathbf{x}_i - \bar{\mathbf{x}})(\mathbf{x}_i - \bar{\mathbf{x}})^T \quad (14)$$

$$W_k = \sum_{q=1}^k \sum_{x \in C_q} (\mathbf{x} - \mathbf{C}_q)(\mathbf{x} - \mathbf{C}_q)^T \quad (15)$$

$$B_k = \sum_{q=1}^k n_q (\mathbf{C}_q - \mathbf{C}_E)(\mathbf{C}_q - \mathbf{C}_E)^T \quad (16)$$

The Silhouette score is an algorithm that clusters datasets into appropriate classes [74]. It assesses individual samples based on two scores and ranges from -1 to +1. The highest score indicates a clear distinction between all classes. Eq. 16 defines the mathematical formulation of the Silhouette score, where  $s$  represents the score,  $a$  represents the mean distance between a sample and other points within the same class, and  $b$  represents the mean distance between a sample and all other points in the nearest cluster [75].

$$s = \frac{b - a}{\max(a, b)} \quad (17)$$

Like previously used metrics, the Davies-Bouldin score employs a clustering algorithm [76,77]. The optimal value for this metric is zero, indicating successful class identification. The Davies-Bouldin score places a strong emphasis on the average similarity between classes. To calculate the Davies-Bouldin score, one can refer to Eq. 17. Here,  $C_i$  ( $i = 1, \dots, k$ ) represents the  $i^{th}$  cluster, while  $C_j$  denotes the most similar cluster to  $C_i$ .  $R_{ij}$ , as shown in Eq. 18, is a trade-off measure representing the within-cluster distance for  $C_i$ . The within-cluster distance, also known as the cluster diameter, is defined as the maximum distance between any two points of a cluster. Finally,  $d_{ij}$  represents the distance between the centroids of  $C_i$  and  $C_j$  [78,79].

$$DB = \frac{1}{k} \sum_{i=1}^k \max_{j \neq i} R_{ij} \quad (18)$$

$$R_{ij} = \frac{s_i + s_j}{d_{ij}} \quad (19)$$

Based on the explanations provided and the results presented in Table 3, it is evident that the DFH algorithm outperformed the other methods. This finding suggests that DFH may be a more practical approach for the given task. According to the Calinski-Harabasz index, the variance ratio of the dataset appears to be appropriate, with a value of 0.892. This result indicates the optimal distribution of variance within the dataset and is significant in assessing the data's suitability for further analysis or interpretation. The Silhouette score is a widely used measure of cluster quality, with a maximum value of 1 indicating optimal clustering. In the context of our implementation, the DFH algorithm achieved a Silhouette score of approximately 0.987, demonstrating strong clustering performance. DFH attained an excellent Davies-Bouldin score of 0.001, highlighting its superior clustering performance.

**Table 3**

The values obtained from calinski-harabasz, silhouette, and davies-bouldin evaluation criteria were used to evaluate all the algorithms under consideration.

Metric Algorithm	Calinski-Harabasz	Silhouette	Davies-Bouldin
Affinity propagation	0.874	0.934	0.011
BIRCH	0.563	0	0.333
DBSCAN	0.823	0.849	0.011
Gaussian mixture	0.643	0.258	0.222
k-means	0.674	0.271	0.222
Mean Shift	0.599	0	0.333
DFH	0.892	0.987	0.001
OPTICS	0.583	0	0.333
Spectral	0.622	0.111	0.222

In order to better understand the performance of all three algorithms, the results have been analyzed objectively. According to the clustering performed by all three clustering algorithms, the hat layer was classified into three categories: old, new, and animals. The shirt layer was divided into two categories, old and new. The face layer was segmented into three groups: sunglasses, eyes, and masks. This classification was finalized for all three algorithms and is output once per engine run. It ensures that when the user selects a specific category objectively, the correct layer is included in the final image.

The results for each algorithm and its classification are given in Table 4. The first column represents the clustering algorithm, the second column shows the layer combinations selected and arranged by the user, and the third column displays the engine's output image. For each algorithm, two-layer configurations were used by the user. The first configuration features a design with an old hat, an old shirt, and pink eyes. The second configuration features a design with a new hat, a new shirt, and a face with sunglasses. As shown in the generated images, only the Deep Fuzzy Hierarchical engine achieved the correct classification accuracy and produced a design that matched the user's layer selections. In the second column, the configurations that executed correctly and the layers placed in the correct categories are bolded. The analysis of the results is also provided in this table, along with an overview of the final design created by the engine.

A comparative evaluation of the three image generation engines is shown in Fig. 10. The evaluation covering DFH, and nine other image generators demonstrates profound differences in their ability to interpret and represent complex layer configurations. When the user configured the layers with the concept of an ice cream cone that includes features like a crown, star-shaped eyes, old clothes, and a yellow background in mind, the recommended DFH engine produced the nearest image, accurately incorporating specified features, including the crown, star-shaped eyes, and old clothing. In contrast, Bing Image Creator failed to generate the "old clothes" aspect, despite successfully applying other elements, showing weaknesses in its semantic grasp of abstract fashion design. Canva, while accurately duplicating the yellow background and crown, rendered the eyes incorrectly by substituting default shapes for the requested stars. These errors highlight the current challenges of generative AI technologies in accurately producing multi-layered and complex artistic designs.

The results emphasize the importance of contextual understanding in artistic creation via AI. DFH's superior performance likely stems from its specialized clustering approach, which keeps more nuanced characteristics of art closer to reality than the commercially offered tools with more general structural frameworks. Canva's absence of clothing textures and Bing's simplification of eye shapes illustrate common failure modes in text-to-image models: either omitting some features or misrepresenting them. Future advancements in generative AI must aim towards fine-grained attribute binding, particularly for hybrid objects (like anthropomorphic food items), where semantic correctness is crucial for artistic believability. This case study shows that even though popular engines excel at wide-level stylistic generation, domain-specialized tools like DFH are advantageous in technically correct and semantically rich creative outputs. However, it should be noted that the proposed model lacks creativity. For example, Aiease, Fotor and Craiyon produce misleading images, but the images are conceptually and visually beautiful.

To summarize and analyze the performance of the DFH method, it should be noted that noisy data usually leads to overlapping clusters. The DFH method, due to its fuzzy feature, classifies noisy data through soft assignment, which results in reduced error. The hierarchical feature enables clusters to be constructed at multiple levels, making the method more robust against random disturbances. These concepts are reflected in the numerical results ( $DB = 0.001$ , Silhouette  $\approx 0.987$ ) and in the practical output (Table 4).

In Fig. 10, the stability of the DFH method under complex and noisy conditions is confirmed. In contrast, general engines such as Bing and

**Table 4**

Final output specific to each algorithm and user's layer configuration.

Algorithm	Order of user	Final result
k-means	<i>First Order</i> Hat: Old (Wrong) Shirt: Old (Right) Face: Eyes (Wrong)	
	<i>Second Order</i> Hat: New (Wrong) Shirt: New (Wrong) Face: Sun glasses (Wrong)	
Deep Fuzzy Hierarchical (DFH)	<i>First Order</i> Hat: Old (Right) Shirt: Old (Right) Face: Eyes (Right)	
	<i>Second Order</i> Hat: New (Right) Shirt: New (Right) Face: Sun glasses (Right)	
Affinity propagation	<i>First Order</i> Hat: Old (Right) Shirt: Old (Right) Face: eyes (Wrong)	

**Table 4 (continued)**

Algorithm	Order of user	Final result
	<i>Second Order</i> Hat: New (Right) Shirt: New (Right) Face: Sun glasses (Wrong)	

Canva produced incorrect renderings for certain descriptions, such as "old clothes" or "star-shaped eyes." This stability is attributed to the fuzzy mechanism, which performs well when handling highly noisy and ambiguous data. Furthermore, the hierarchical nature of the clusters across multiple levels provides greater resistance to randomness in layer structuring. The qualitative results, together with the numerical analyses ( $DB = 0.001$ , Silhouette  $\approx 0.987$ ), demonstrate the superiority of DFH in accuracy and semantic consistency when the data is noisy.

## 5. Discussion

The proposed engine utilizes a personal dataset and implements clustering on its layers to generate NFT artwork, setting it apart from most recent works that utilize GANs for image production. A significant limitation of artificial intelligence, is the absence of a soul in the design. AI-driven art can lack the depth and intent that human-generated art carries, which presents a challenge. The creation of a meaningful dataset was a complex task, requiring specialized artistic knowledge and expertise. Consequently, the final designs and images generated through this research carry both practical and entertainment value but remain limited in creativity.

One of the challenges in AI-driven image processing is how to combine image layers while preserving artistic nuance. When relying purely on automated commands, the artistic depth can often be lost. To address this, we involved artists in the creation of the dataset, allowing for a more hands-on approach. The images were then generated using clustering methods, which helped to maintain the artistic integrity of the work. As a result, the images produced not only hold commercial potential in the NFT market but also reflect genuine artistic expression. To ensure the quality and authenticity of the designs, we drew from extensive studies in fine arts, integrating this knowledge into the creation process.

While we cannot claim to have solved the problem of imbuing AI-generated art with a soul," we have made progress in opening a new intersection between AI and fine arts. Our findings suggest that combining expert-curated datasets with AI can partially address the gap between automated art generation and true artistic creativity. However, as it stands, the engine requires manual intervention for arranging and selecting image layers, with the system randomly generating the artwork. This makes the current version of the software limited in terms of flexibility, as it does not yet utilize Large Language Models (LLMs) for interpreting user input.

While the current system demonstrates valuable functionality, it also operates under several practical constraints. Our manual curation process for our collection ensures quality but introduces system scalability limitations. Introducing new content into the art requires a considerable amount of time from trained artists, hence limiting large-scale deployment. The clustering algorithm we employed, while satisfactory for our proof-of-concept, suffers from performance lag when handling intricate artistic styles with small changes, a common issue in computational art analysis.

Engine	Output	Engine	Output
DFH		PIXLR	
Bing Image Creator		Aicase	
Canva		Magic Studio	
Gen craft		Leonardo.Ai	
Craiyon		Fotor	

**Fig. 10.** Objective comparison of the outputs from nine well-known engines, alongside the proposed DHF engine, based on the user configuring the layers with the concept of an ice cream cone that has a crown, star-shaped eyes, old clothes, and a yellow background in mind.

Several limitations in the current implementation also point to areas for future work. First, we aim to develop interactive software tools that allow artists to conveniently contribute to and annotate the dataset. Second, we plan to test other machine learning techniques, such as self-organizing maps that may better describe artistic correspondence. Third, conducting cross-disciplinary testing with working artists will be essential to assess usability and the practical impact of our method. Additionally, the incorporation of LLMs into our software will be a key focus in future versions, allowing the system to understand and generate artwork based on user-written prompts, which will make the creation process more intuitive and flexible. The method could also be extended to other forms of art, like musical composition or architectural design, though this would require extensive alteration. Such applications would inevitably raise profound questions about creative ownership, which are worthy of separate ethical consideration.

## 6. Conclusion

The present study aimed to develop an engine for generating Non-fungible token (NFT) images, focusing on addressing various challenges within the fields of information technology and software development through artificial intelligence (AI). To achieve this objective, datasets were created by generating diverse image layers, and specific categories of these layers were established using clustering algorithms. NFT artwork was subsequently produced by allowing users to select their preferred layers and specify the desired number of images.

In the results section, the Deep Fuzzy Hierarchical Clustering algorithm was employed to classify the image layers, achieving an accuracy rate exceeding 90 % and yielding satisfactory images across multiple trials. Several factors pose limitations to the research scope of digital

imagery, including the necessity for a personalized dataset, the influence of market dynamics and non-artistic viewpoints, as well as the lack of artistic elements in AI-generated content.

To address these challenges, future developments of the NFT-AGE engine can be considered, emphasizing the importance of investing in artists' efforts to produce multiple image layers in order to establish a comprehensive database. Additionally, further examination and evaluation of machine learning techniques may enhance the proposed engine's performance. For instance, optimizing clustering parameters could be targeted as a future endeavor, employing hyper-heuristic algorithms for improved outcomes in the realm of IT and software solutions.

## CRediT authorship contribution statement

**Arman Daliri:** Writing – original draft, Visualization, Validation, Supervision, Software, Resources, Project administration, Methodology, Investigation, Formal analysis, Data curation, Conceptualization. **Nora Mahdavi:** Writing – review & editing, Visualization, Validation, Software, Methodology, Investigation, Formal analysis, Conceptualization. **Nima Zaeimzadeh:** Visualization, Software, Methodology, Data curation, Conceptualization. **Mahdieh Zabihimayvan:** Writing – review & editing, Validation, Supervision, Methodology, Investigation, Conceptualization. **Aynaz Norouzi Barhangar:** Writing – original draft, Visualization, Validation, Resources, Investigation, Formal analysis, Data curation. **Mohammadzadeh Javad:** Validation, Supervision, Project administration.

## Ethical approval

This research did not interfere with ethical laws, and accessible sources were used.

## Code availability

The software's MVP (Minimum Viable Product) version is provided for demonstration purposes [80], allowing users to view the output.

## Funding

No funding was received for conducting this study.

## Declaration of Competing Interest

There are no competitive resources or financial relationships in the creation of this research, and all authors participated in this research voluntarily.

## Data availability

Data will be made available on request.

## References

- [1] F. Hayashi, A. Routh, Financial literacy, risk tolerance, and cryptocurrency ownership in the United States, *J. Behav. Exp. Financ.* (2025) 101060. (<https://www.sciencedirect.com/science/article/pii/S2214635025000413>) (accessed August 26, 2025).
- [2] M. Ali, S. Bagui, Introduction to NFTs: the future of digital collectibles, *Int. J. Adv. Comput. Sci. Appl.* 12 (2021) 50–56.
- [3] M. Nadini, L. Alessandretti, F. Di Giacinto, M. Martino, L.M. Aiello, A. Baronchelli, Mapping the NFT revolution: market trends, trade networks, and visual features, *Sci. Rep.* 11 (2021) 20902.
- [4] S.M.H. Bamakan, N. Nezhadsistani, O. Bodaghi, Q. Qu, Patents and intellectual property assets as non-fungible tokens; key technologies and challenges, *Sci. Rep.* 12 (2022) 1–13.
- [5] T. Wang, A Deep Learning-Based programming and creation algorithm of NFT artwork, *Mob. Inf. Syst.* 2022 (2022).
- [6] N. Farooq, S. Bashir, A.A. Banka, A.M. Malla, H. Manzoor, M. Farooq, Blockchain architecture and development process, in: K. Ahmad, U.N. Dulhare, M.S. Badar, J. Ahmed, M.A. Rizvi (Eds.), *Foster. Mach. Learn. IoT Blockchain Technol.*, Springer Nature Singapore, Singapore, 2025, pp. 115–161, [https://doi.org/10.1007/978-981-96-4078-2\\_4](https://doi.org/10.1007/978-981-96-4078-2_4).
- [7] J. Kävrestad, M. Birath, N. Clarke, Fundamentals of digital forensics: a guide to theory, *Research and Applications*, Springer International Publishing, Cham, 2024, <https://doi.org/10.1007/978-3-031-53649-6>.
- [8] M. Alimoradi, M. Zabihimayvan, A. Daliri, R. Sledzik, R. Sadeghi, Deep neural classification of darknet traffic, in: A. Cortés, F. Grimaldo, T. Flaminio (Eds.), *Front. Artif. Intell. Appl.*, IOS Press, 2022, <https://doi.org/10.3233/FAIA220323>.
- [9] S. Shahriar, K. Hayawi, NFTGAN: Non-Fungible token art generation using generative adversarial networks, in: 2022 7th Int. Conf. Mach. Learn. Technol. ICLMT, ACM, Rome Italy, 2022, pp. 255–259, <https://doi.org/10.1145/3529399.3529439>.
- [10] M.M. Soliman, E. Ahmed, A. Darwish, A.E. Hassanien, Artificial intelligence powered metaverse: analysis, challenges and future perspectives, *Artif. Intell. Rev.* 57 (2024) 36, <https://doi.org/10.1007/s10462-023-10641-x>.
- [11] E. Cetinic, J. She, Understanding and creating art with AI: review and outlook, *ACM Trans. Multimed. Comput. Commun. Appl.* 18 (2022) 66:1–66:22, <https://doi.org/10.1145/3475799>.
- [12] A. Chebli, S. Cherbal, Building a secure and efficient NFT marketplace: AI integration, lazy minting, and trustguard, *Int. J. Inf. Secur.* 24 (2025) 140, <https://doi.org/10.1007/s10207-025-01056-6>.
- [13] A. Babaei, E.B. Tirkolaei, E. Boz, Optimizing energy consumption for blockchain adoption through renewable energy sources, *Renew. Energy* 238 (2025) 121936. (<https://www.sciencedirect.com/science/article/pii/S0960148124020044>) (accessed August 26, 2025).
- [14] W.J.-W. Tann, A. Vuputuri, E.-C. Chang, Projecting Non-Fungible Token (NFT) Collections: A Contextual Generative Approach,(2023). (Accessed March 8, 2024), <http://arxiv.org/abs/2210.15493>.
- [15] E. ŞAHİN, N.N. Arslan, D. Özdemir, Unlocking the black box: an in-depth review on interpretability, explainability, and reliability in deep learning, *Neural Comput. Appl.* 37 (2025) 859–965, <https://doi.org/10.1007/s00521-024-10437-2>.
- [16] Z. Dafir, Y. Lamari, S.C. Slaoui, A survey on parallel clustering algorithms for big data, *Artif. Intell. Rev.* 54 (2021) 2411–2443, <https://doi.org/10.1007/s10462-020-09918-2>.
- [17] A. Daliri, M. Alimoradi, M. Zabihimayvan, R. Sadeghi, World Hyper-Heuristic: a novel reinforcement learning approach for dynamic exploration and exploitation, *Expert Syst. Appl.* 244 (2024) 122931. (<https://www.sciencedirect.com/science/article/pii/S0957417423034334>) (Accessed January 9, 2024).
- [18] G.B. Meisner, The golden ratio: The divine beauty of mathematics, Race Point Publishing, 2018. (Accessed August 26, 2025) ([https://books.google.com/books?hl=en&lr=&id=9SI1DwAAQBAJ&oi=fnd&pg=PP1&ots=4XsLOMNt&sig=yLpDSAOj\\_YoAW3FYBaVhChZiOKI](https://books.google.com/books?hl=en&lr=&id=9SI1DwAAQBAJ&oi=fnd&pg=PP1&ots=4XsLOMNt&sig=yLpDSAOj_YoAW3FYBaVhChZiOKI)).
- [19] A. Palmer, Neoclassicism and Religious Art, in: Oxf. Res. Encycl. Relig., 2021. (Accessed August 26, 2025) (<https://oxfordre.com/religion/display/10.1093/acrefore/9780199340378.001.0001/acrefore-9780199340378-e-903>).
- [20] A.J. Eddy, Cubists and Post-impressionism, AC McClurg & Company, 1914. (Accessed August 26, 2025) (<https://books.google.com/books?hl=en&lr=&id=LpAEAAAAYAAJ&oi=fnd&pg=PA1&ots=vQIyy-V-OR&sig=YC67j2xkvTaT08J6mijY33-nghQ>).
- [21] Y. Song, The analysis of the vision of the sermon: a comparative study on Gauguin's relationship with symbolism and fauvism, *J. Educ. Humanit. Soc. Sci.* 1 (2022) 308–314.
- [22] N. Wolf, U. Grosenick, Expressionism, Taschen, 2004. (Accessed August 26, 2025) (<https://books.google.com/books?hl=en&lr=&id=MbOdSrOFfpEC&oi=fnd&pg=PA6&ots=DDJUR9MDNV&sig=Q6F-Nw1ENgoGAJVqxFy2mN7CWI>).
- [23] C. Raschke, Evangelicals in the public square, *Society* 46 (2009) 147–154, <https://doi.org/10.1007/s12115-008-9176-3>.
- [24] P. Virilio, The futurism of the instant: Stop-eject, Polity, 2010. (Accessed August 26, 2025) (<https://books.google.com/books?hl=en&lr=&id=f5720Xb9aUkC&oi=fnd&pg=PR1&ots=Bd5ZB-dpFS&sig=EPrE318QZ9rmq73JuwkSs2Y7CLw>).
- [25] E. Doss, Benton, pollock, and the politics of modernism: from regionalism to abstract expressionism, University of Chicago Press, 1995.
- [26] O. Lizardo, S. Skiles, Cultural consumption in the fine and popular arts realms, *Sociol. Compass* 2 (2008) 485–502, <https://doi.org/10.1111/j.1751-9020.2008.00101.x>.
- [27] D. Blaiklock, What is the nature of illustration expertise? in: A. Male (Ed.), *Companion Illus.*, 1st ed Wiley, 2019, pp. 185–198, <https://doi.org/10.1002/9781119185574.ch8>.
- [28] T. Crow, T.E. Crow, Modern art in the common culture, Yale University Press, 1996. ([https://books.google.com/books?hl=en&lr=&id=ugP\\_59ogKDCi&oi=fnd&pg=PR7&ots=-YDJUTvF4c&sig=Y9tTZvk9gioA9n9RJiaAMjgjXKWo](https://books.google.com/books?hl=en&lr=&id=ugP_59ogKDCi&oi=fnd&pg=PR7&ots=-YDJUTvF4c&sig=Y9tTZvk9gioA9n9RJiaAMjgjXKWo)) (Accessed August 27, 2025).
- [29] N. Malik, G. Appel, L. Luo, Blockchain technology for creative industries: current state and research opportunities, *Int. J. Res. Mark.* 40 (2023) 38–48. (<https://www.sciencedirect.com/science/article/pii/S0167811622000544>) (Accessed August 27, 2025).
- [30] K. Vasan, M. Janosov, A.-L. Barabási, Quantifying NFT-driven networks in crypto art, *Sci. Rep.* 12 (2022) 2769. (<https://www.nature.com/articles/s41598-022-05146-6>) (Accessed August 27, 2025).
- [31] D. Kim, M.J. Lee, W. Ki, D. Kim, Exploring the role of User-Driven communities in NFT valuation: a case study of discord, *J. Multimed. Inf. Syst.* 9 (2022) 299–314. (<https://www.jmis.org/archive/view.article?pid=jmis-9-4-299>) (Accessed August 27, 2025).
- [32] R. Belk, M. Humayun, M. Brouard, Money, possessions, and ownership in the metaverse: NFTs, cryptocurrencies, Web3 and wild markets, *J. Bus. Res.* 153 (2022) 198–205. (<https://www.sciencedirect.com/science/article/pii/S0148296322007147>) (Accessed August 27, 2025).
- [33] E.B. Silva, Distinction through visual art, *Cult. Trends* 15 (2006) 141–158, <https://doi.org/10.1080/09548960600712942>.
- [34] J. Bateman, Text and image: a critical introduction to the visual/verbal divide, Routledge, 2014. (<https://www.taylorfrancis.com/books/mono/10.4324/978131573971/text-image-john-bateman>) (Accessed August 27, 2025).
- [35] P.O. Kristeller, The modern system of the arts: a study in the history of aesthetics (II), *J. Hist. Ideas* (1952) 17–46. (<https://www.jstor.org/stable/2707724>) (Accessed January 27, 2024).
- [36] M.H. Bogart, Artists, advertising, and the borders of art, University of Chicago Press, 1995. (<https://books.google.com/books?hl=en&lr=&id=Gw5QvFTS6vAC&oi=fnd&pg=PR9&ots=U3cULLKIHW&sig=7RQoD9LwVJlk2yyA6f88a7Der8s>) (Accessed August 27, 2025).
- [37] D. Howes, In the balance: the art of norman rockwell and alex colville as discourses on the constitutions of the United States and Canada, *Alta Rev.* 29 (1991) 475. ([https://heinonline.org/hol-cgi-bin/get\\_pdf.cgi?handle=hein.journals/alblr29&section=27](https://heinonline.org/hol-cgi-bin/get_pdf.cgi?handle=hein.journals/alblr29&section=27)) (Accessed January 27, 2024).
- [38] A. Gomez-Cabrera, P.J. Escamilla-Ambrosio, J. Happa, ViLanIoT: a visual language for improving Internet of things systems representation, *J. Ind. Inf. Integr.* (2024) 100567. (<https://www.sciencedirect.com/science/article/pii/S2452414X24000116>) (Accessed January 27, 2024).
- [39] A. Efland, Art and cognition: integrating the visual arts in the curriculum, Teachers College Press, 2002. (<https://books.google.com/books?hl=en&lr=&id=DhUuYYd4O4AC&oi=fnd&pg=PR7&dq=While+both+fall+under+the+umbrella+of+visual+arts,+there+are+distinct+differences+between+Illustration+and+fine+arts.&ots=2nKgSFYA7&sig=z18FaZ1efZK8UfpQl92934Ycamo>) (Accessed January 27, 2024).
- [40] M. Nienhaus, J. Dollner, Depicting dynamics using principles of visual art and narrations, *IEEE Comput. Graph. Appl.* 25 (2005) 40–51. (<https://ieeexplore.ieee.org/abstract/document/1438257/>) (Accessed August 27, 2025).
- [41] C.T. Lee, Y.-C. Shen, Z. Li, H.-H. Xie, The effects of non-fungible token platform affordances on customer loyalty: a Buyer-Creator duality perspective, *Comput. Hum. Behav.* 151 (2024) 108013. (<https://www.sciencedirect.com/science/article/pii/S0747563223003643>) (Accessed January 27, 2024).

- [42] C.-H. Wu, C.-Y. Liu, T.-S. Weng, Critical factors and trends in NFT technology innovations, *Sustainability* 15 (2023) 7573. (<https://www.mdpi.com/2071-1050/15/9/7573>) (Accessed August 27, 2025).
- [43] R. Moncada, E. Ferro, A. Favenza, P. Freni, Next generation Blockchain-Based financial services, in: B. Balis, D.B. Heras, L. Antonelli, A. Bracciali, T. Gruber, J. Hyun-Wook, M. Kuhn, S.L. Scott, D. Unat, R. Wyrzykowski (Eds.), *Euro-Par 2020 Parallel Process. Workshop*, Springer International Publishing, Cham, 2021, pp. 30–41, [https://doi.org/10.1007/978-3-030-71593-9\\_3](https://doi.org/10.1007/978-3-030-71593-9_3).
- [44] H.-J. Lim, S. Lee, M. Kim, W. LeeComparative analysis of security features and risks in digital asset wallets 14 *Electronics*2025, 2436(Accessed August 27, 2025)(<http://www.mdpi.com/2079-9292/14/12/2436>).
- [45] B. Jenkins, NFTs and the financialization of art, *Cult. Stud.* 39 (2025) 626–655, <https://doi.org/10.1080/09502386.2024.2329873>.
- [46] M. Nour, J.P. Chaves-Ávila, Á. Sánchez-Miralles, Review of blockchain potential applications in the electricity sector and challenges for large scale adoption, *IEEE Access* 10 (2022) 47384–47418. (<https://ieeexplore.ieee.org/abstract/document/9765489/>) (accessed January 27, 2024).
- [47] E. Cho, G. Jensen, Y. Yoo, A. Mahanti, J.-K. Kim, Characterizing the initial and subsequent NFT sales market dynamics: perspectives from boom and slump periods, *IEEE Access* 12 (2023) 3638–3658. (<https://ieeexplore.ieee.org/abstract/document/10320355/>) (Accessed August 27, 2025).
- [48] H.E. Zainab, N.Z. Bawany, J. Imran, W. Rehman, Virtual dimension—a primer to metaverse, *IT Prof.* 24 (2022) 27–33. (<https://ieeexplore.ieee.org/abstract/document/10017431/>) (Accessed March 8, 2024).
- [49] M.M. Alshater, N. Nasrallah, R. Khouri, M. Joshipura, Deciphering the world of NFTs: a scholarly review of trends, challenges, and opportunities, *Electron. Commer. Res.* (2024), <https://doi.org/10.1007/s10660-024-09881-y>.
- [50] A. Obukhov, M. Krasnyanskiy, Quality assessment method for GAN based on modified metrics inception score and Fréchet inception distance, in: R. Silhavy, P. Silhavy, Z. Prokopova (Eds.), *Softw. Eng. Perspect. Intell. Syst.*, Springer International Publishing, Cham, 2020, pp. 102–114, [https://doi.org/10.1007/978-3-030-63322-6\\_8](https://doi.org/10.1007/978-3-030-63322-6_8).
- [51] L.-H. Lee, Z. Lin, R. Hu, Z. Gong, A. Kumar, T. Li, S. Li, P. Hui, When creators meet the metaverse: A survey on computational arts, *ArXiv Prepr. ArXiv211113486* (2021).
- [52] A. Dash, J. Ye, G. Wang, A review of generative adversarial networks (GANs) and its applications in a wide variety of disciplines: from medical to remote sensing, *IEEE Access* 12 (2024) 18330–18357, <https://doi.org/10.1109/ACCESS.2023.3346273>.
- [53] Z. Qin, Z. Liu, P. Zhu, Y. Xue, A GAN-based image synthesis method for skin lesion classification, *Comput. Methods Prog. Biomed.* 195 (2020) 105568. (<https://www.sciencedirect.com/science/article/pii/S0169260720302418>) (Accessed August 27, 2025).
- [54] A.A. Nayak, P.S. Venugopala, B. Ashwini, A systematic review on generative adversarial network (GAN): challenges and future directions, *Arch. Comput. Methods Eng.* 31 (2024) 4739–4772, <https://doi.org/10.1007/s11831-024-10119-1>.
- [55] V.L. Trevisan de Souza, B.A.D. Marques, H.C. Batagelo, J.P. Gois, A review on generative adversarial networks for image generation, *Comput. Graph* 114 (2023) 13–25, <https://doi.org/10.1016/j.cag.2023.05.010>.
- [56] M. Alimoradi, R. Sadeghi, A. Daliri, M. Zabihimayyan, Statistic deviation mode balancer (SDMB): a novel sampling algorithm for imbalanced data, *Neurocomputing* (2025) 129484. (<https://www.sciencedirect.com/science/article/pii/S0925231225001560>) (Accessed January 28, 2025).
- [57] A. Daliri, M. Khalilian, J. Mohammadzadeh, S.S. Hosseini, Optimized active fuzzy deep federated learning for predicting autism spectrum disorder, *Netw. Model. Anal. Health Inform. Bioinforma.* 14 (2025), <https://doi.org/10.1007/s13721-025-00523-3>.
- [58] V. Snášel, M. Štěpníčka, V. Ojha, P.N. Suganthan, R. Gao, L. Kong, Large-scale data classification based on the integrated fusion of fuzzy learning and graph neural network, *Inf. Fusion* 102 (2024) 102067. (<https://www.sciencedirect.com/science/article/pii/S1566253523003834>) (Accessed March 8, 2024).
- [59] Q. Ou, S. Wang, P. Zhang, S. Zhou, E. Zhu, Anchor-based multi-view subspace clustering with hierarchical feature descent, *Inf. Fusion* 106 (2024) 102225. (<https://www.sciencedirect.com/science/article/pii/S1566253524000034>) (Accessed March 8, 2024).
- [60] A. Daliri, R. Sadeghi, N. Sedighian, A. Karimi, J. Mohammadzadeh, Heptagonal reinforcement learning (HRL): a novel algorithm for early prevention of non-sinus cardiac arrhythmia, *J. Ambient Intell. Humaniz. Comput.* 15 (2024) 2601–2620, <https://doi.org/10.1007/s12652-024-04776-0>.
- [61] A. Daliri, A. Asghari, H. Azgomi, M. Alimoradi, The water optimization algorithm: a novel metaheuristic for solving optimization problems, *Appl. Intell.* 52 (2022) 17990–18029, <https://doi.org/10.1007/s10489-022-03397-4>.
- [62] S. Harifi, M. Khalilian, J. Mohammadzadeh, S. Ebrahimpnejad, Using metaheuristic algorithms to improve k-Means clustering: a comparative study, *Rev. Intell. Artif.* 34 (2020). ([https://www.academia.edu/download/64125978/34.03\\_07.pdf](https://www.academia.edu/download/64125978/34.03_07.pdf)) (Accessed April 13, 2025).
- [63] C.-D. Wang, J.-H. Lai, C.Y. Suen, J.-Y. Zhu, Multi-exemplar affinity propagation, *IEEE Trans. Pattern Anal. Mach. Intell.* 35 (2013) 2223–2237. (<https://ieeexplore.ieee.org/abstract/document/6420838/>) (accessed August 27, 2025).
- [64] S. Anand, S. Mittal, O. Tuzel, P. Meer, Semi-supervised kernel mean shift clustering, *IEEE Trans. Pattern Anal. Mach. Intell.* 36 (2013) 1201–1215. (<https://ieeexplore.ieee.org/abstract/document/6616555/>) (Accessed August 27, 2025).
- [65] U. Von Luxburg, A tutorial on spectral clustering, *Stat. Comput.* 17 (2007) 395–416, <https://doi.org/10.1007/s11222-007-9033-z>.
- [66] D. Deng, DBSCAN clustering algorithm based on density. in: 2020 7th Int. Forum Electr. Eng. Autom. IFEEA, IEEE, 2020, pp. 949–953. (<https://ieeexplore.ieee.org/abstract/document/9356727/>) (Accessed January 27, 2024).
- [67] M. Ankerst, M.M. Breunig, H.-P. Kriegel, J. Sander, OPTICS: ordering points to identify the clustering structure, *ACM SIGMOD Rec.* 28 (1999) 49–60, <https://doi.org/10.1145/304181.304187>.
- [68] Z. He, C.-H. Ho, An improved clustering algorithm based on finite Gaussian mixture model, *Multimed. Tools Appl.* 78 (2019) 24285–24299, <https://doi.org/10.1007/s11042-018-6988-z>.
- [69] T. Zhang, R. Ramakrishnan, M. Livny, BIRCH: a new data clustering algorithm and its applications, *Data Min. Knowl. Discov.* 1 (1997) 141–182, <https://doi.org/10.1023/A:1009783824328>.
- [70] A. Daliri, M. Khoshbakhti, M.K. Samadi, M. Rahiminia, M. Zabihimayyan, R. Sadeghi, Equilateral active learning (EAL): a novel framework for predicting autism spectrum disorder based on active fuzzy federated learning. in: *Artif. Intell. Soc. Comput.*, AHFE Open Acces, 2024, <https://doi.org/10.54941/ahfe1004655>.
- [71] A. Mohammadifar, H. Samadbin, A. Daliri, Accurate Autism Spectrum Disorder prediction using Support Vector Classifier based on Federated Learning (SVCLF), *ArXiv Prepr. ArXiv231104606* (2023). (Accessed October 2, 2024)(<https://arxiv.org/abs/2311.04606>).
- [72] K.P. Sinaga, M.-S. Yang, Unsupervised K-means clustering algorithm, *IEEE Access* 8 (2020) 80716–80727.
- [73] X. Wang, Y. Xu, An improved index for clustering validation based on silhouette index and Calinski-Harabasz index. in: *IOP Conf. Ser. Mater. Sci. Eng.*, IOP Publishing, 2019 052024.
- [74] L. Lovmar, A. Ahlford, M. Jonsson, A.-C. Syvänen, Silhouette scores for assessment of SNP genotype clusters, *BMC Genom.* 6 (2005) 35, <https://doi.org/10.1186/1471-2164-6-35>.
- [75] A. Daliri, M. Zabihimayyan, K. Saleh, Vector result rate (VRR): a novel method for fraud detection in mobile payment systems. in: *Artif. Intell. Soc. Comput.*, AHFE Open Acces, 2024, <https://doi.org/10.54941/ahfe1004641>.
- [76] J. Xiao, J. Lu, X. Li, Davies bouldin index based hierarchical initialization K-means, *Intell. Data Anal.* 21 (2017) 1327–1338.
- [77] A. Daliri, K. Branch, M. Sheikha, K.K. Roudposhti, L. Branch, M. Alimoradi, J. Mohammadzadeh, Optimized Categorical Boosting for Gastric Cancer Classification using Heptagonal Reinforcement learning and the Water Optimization Algorithm, (n.d.).(Accessed March 6, 2025) ([https://www.researchgate.net/profile/Arman-Daliri/publication/389465487\\_Optimized\\_Categorical\\_Boosting\\_for\\_Gastric\\_Cancer\\_Classification\\_using\\_Heptagonal\\_Reinforcement\\_learning\\_and\\_the\\_Water\\_Optimization\\_Algorithm/links/67c3173f645ef274a4988598/Optimized-Categorical-Boosting-for-Gastric-Cancer-Classification-using-Heptagonal-Reinforcement-learning-and-the-Water-Optimization-Algorithm.pdf](https://www.researchgate.net/profile/Arman-Daliri/publication/389465487_Optimized_Categorical_Boosting_for_Gastric_Cancer_Classification_using_Heptagonal_Reinforcement_learning_and_the_Water_Optimization_Algorithm/links/67c3173f645ef274a4988598/Optimized-Categorical-Boosting-for-Gastric-Cancer-Classification-using-Heptagonal-Reinforcement-learning-and-the-Water-Optimization-Algorithm.pdf)).
- [78] D.L. Davies, D.W. Bouldin, A cluster separation measure, *IEEE Trans. Pattern Anal. Mach. Intell.* (1979) 224–227.
- [79] M. Halkidi, Y. Batistakis, M. Vazirgiannis, On clustering validation techniques, *J. Intell. Inf. Syst.* 17 (2001) 107–145.
- [80] NimaZaeim, NimaZaeim/NFT-AGE, (2025). (Accessed April 23, 2025) (<https://github.com/NimaZaeim/NFT-AGE>).



**Dr. Arman Daliri** received a B.S Degree in Software Engineering from the Computer Engineering Faculty at Islamic Azad University. He received an M.Sc. in artificial intelligence and robotics from the Computer Engineering Faculty at Shahrood Institute of Higher Education, Tonekabon, Iran. He is now an Instructor and Consultant of the KIAU Research and Technology Advisory Council at the Islamic Azad University Karaj Branch, which works on machine learning and artificial intelligence in health care. His research interests include Optimization algorithms, evolutionary computing, and machine learning.



**Nora Mahdavi** is a Computer Engineering student at Azad University, Karaj Branch, studying from 2022 to 2025. She is an aspiring data scientist focusing on analyzing complex datasets to extract meaningful insights and create clear, actionable visualizations. Nora is particularly passionate about leveraging AI and machine learning in healthcare, with the goal of conducting research to develop predictive models and innovative solutions for cancer diagnosis.



**Dr. Mahdieh Zabihimayvan** is an assistant professor of Computer Science at Central Connecticut State University. She works on the applications of artificial intelligence for cybersecurity and sociotechnical systems with the aim of improving proactive cyber threat intelligence applications in protecting privacy of Internet users.



**Nima Zaeimzadeh** is a highly motivated UI/UX Designer with two years of freelancing experience in developing projects across mobile applications, web design, AI platforms, and e-commerce. He is eager to explore new design trends and continuously refine his style. Proficient in Figma and Framer, he stays up to date with modern design systems and has additional experience with Photoshop. This expertise allows him to craft intuitive and visually appealing user interfaces that enhance the overall user experience. Currently, he is pursuing a master's degree to further expand his knowledge.



**Aynaz Norouzi Baranghar** is a painting student at the Faculty of Fine Arts, University of Tehran, where she has been studying since 2021. With a passion and enthusiasm for visual arts, she strives to create innovative and unique works by utilizing various techniques and styles of painting. Aynaz's main expertise in the field of painting positions her as a young and emerging artist in this domain.



**Dr. Javad Mohammadzadeh** received the B.Sc. degree in computer science from Shahid Bahonar University of Kerman, Kerman, Iran, in 2004, and the M.Sc. degree in computer science and the Ph.D. degree in bioinformatics from the University of Tehran, Tehran, Iran, in 2007 and 2014, respectively. He is an Associate Professor with the Software Engineering Department, Islamic Azad University, Karaj Branch, Iran. His current research interests include swarm intelligence algorithms, bioinformatics algorithms, complex dynamical networks, and parallel computing.